



Uranium(VI) adsorption and surface complexation modeling onto vadose sediments from the Savannah River Site

F. M. Coutelot¹ · J. C. Seaman¹ · M. Baker¹

Received: 13 December 2016 / Accepted: 30 January 2018 / Published online: 17 February 2018
© Springer-Verlag GmbH Germany, part of Springer Nature 2018

Abstract

Uranium U(VI) adsorption was measured as function of pH (3–10) on goethite, kaolinite, quartz, two binary mixtures of goethite and kaolinite, and a vadose zone sediment collected on The Department of Energy's Savannah River Site (SRS), the clay mineral fraction of which is composed largely of kaolinite and goethite. Diffuse-layer surface complexation models were parameterized using the code PEST together with PHREEQC to fit U(VI) sorption data for the pure goethite, kaolinite, and quartz. U(VI) adsorption on kaolinite and goethite was modeled as the formation of two bidentate U(VI) complexes at mineral edge sites on a variable charge site. U(VI) adsorption on quartz was described using a one-site diffuse-layer with the formation of bidentate complex on a variable charge site. These models were used to predict U(VI) adsorption on the binary sorbent mixtures and the SRS sediment using a simple component-additivity approach. In general, the predicted adsorption edges were in good agreement with measured data, with statistically similar goodness of fit compared to that obtained for the pure mineral systems.

Keywords Uranium sorption · Surface complexation modeling · Zeta potential · Goethite · PHREEQC · PEST

Introduction

The Department of Energy's Savannah River Site (SRS) near Aiken, South Carolina (SC) includes several (former) nuclear facilities for the production and refinement of materials for nuclear weapons. As a result of SRS operations, uranium (U) and other contaminants have entered the surrounding environment through accidental and purposeful discharges (Li et al. 2014). Uranium is also the most common contaminant found throughout the DOE complex (Riley et al. 1992). Following many years of active site remediation focused on removing much of the remaining contaminant source term, there is a strong demand to assess the continued migration behavior of U in the soils and sediments underlying the SRS. It has become increasingly apparent over recent years that a mechanistic understanding of sorption processes and the development of accurate predictive sorption models are necessary to properly justify and defend environmental management and remediation decisions.

The chemistry of U is complex, such that small changes in solution chemistry can have a large change in chemical speciation and solid phase partitioning. The most common and mobile form of U under oxidized conditions is the U(VI) uranyl ion, UO_2^{2+} . The mobility of U(VI) in the subsurface is highly dependent on pH (Uyuşur et al. 2014), redox potential, ionic strength (Bachmaf and Merkel 2010), and the presence of aqueous or surface ligands containing C, Fe, P, S, and Si (Waite et al. 1994; Jerden Jr. et al. 2003; Cheng et al. 2004; Fox et al. 2006). At neutral pH, U primarily exists as soluble U(VI) species under oxidizing conditions or as less soluble U(IV) species under reducing conditions (O'Loughlin et al. 2011). Under oxidizing conditions and neutral pH, U(VI) species can be immobilized by adsorption to iron oxyhydroxides (Li and Kaplan 2012). Under reducing conditions, U(VI) can be reduced to immobile U(IV) chemically by reduced iron- or sulfur-surface species (Hyun et al. 2009; Chang et al. 2014) and/or biologically by native anaerobic microbial communities (Tapia-Rodríguez et al. 2012).

Uranium sorption on various mineral phases has been widely described in the literature (Waite et al. 1994; Arnold et al. 1998; Barnett et al. 2000; Arnold et al. 2001; Prikryl et al. 2001; Um et al. 2008; Hyun et al. 2009; Mahoney

✉ F. M. Coutelot
coutelot@uga.edu

¹ Savannah River Ecology Laboratory, University of Georgia, Aiken, SC 29802, USA

et al. 2009; Bachmaf and Merkel 2010; Stoliker et al. 2011; Dong et al. 2012; Nair et al. 2014; Uyuşur et al. 2014; Wang et al. 2015). A range of geochemical processes, including dissolution/precipitation reactions, ion exchange, and redox transformations at the water–mineral interface, control the mobility and transport of U in the subsurface systems such as soils, and vadose- and saturated-zone sediments (Bachmaf and Merkel 2010). Sorption is the dominant factor affecting U(VI) mobility in oxidized subsurface environments. However, the dependence of sorption on a range of aqueous solution properties (i.e., pH, E_h , total U concentration, ionic strength, competing ions, and presence of complexing ligands) and the physicochemical characteristics of the sorbing material (i.e., mineral compositions, surface area, density of sorptive surface sites, solid/solution ratio, etc.) makes the prediction of U(VI) retardation and transport difficult in natural geologic systems that are both physically and chemically heterogeneous (Arnold et al. 2001; Prikryl et al. 2001; Davis et al. 2004; Payne et al. 2004; Nair et al. 2014; Dong and Wan 2014).

Contaminant partitioning is usually described in a simplistic manner within chemical transport codes using the empirical K_d method in which a distribution equilibrium between solid and aqueous phases is assumed. This approach, however, ignores the chemical speciation of the contaminant in solution and at the mineral–water interface, yielding results that are generally valid only for the specific solution conditions for which the K_d value was derived. More recently the interactions of dissolved ionic species with the mineral–water interface have been interpreted and quantified using more specific surface complexation models (SCMs) (Bradbury and Baeyens 2009). SCMs describe the formation of surface species based on the aqueous chemical speciation of the sorbate and reactions between discrete surface functional groups, while also accounting for the influence of electrostatic potentials resulting from amphoteric reactions at the mineral surface (Davis et al. 2004). Surface complexation modeling has emerged as powerful tool for describing adsorption processes under varying geochemical conditions (Payne et al. 2004; Davis et al. 2004; Bachmaf and Merkel 2010; Dong et al. 2012).

There are two major approaches for applying SCM to natural materials: the component additivity (CA) and the generalized composite (GC) approaches (Davis et al. 2004). The GC approach was developed as a means of describing solute adsorption on complex sediments and/or soils, assuming that natural sorbent materials are far too heterogeneous and complex to be described by a limited set of specific idealized minerals, and even reactive organic components, in part because of our limited understanding of the electrical double layer in complex mineral systems (Davis et al. 1998; Davis 2003). The GC approach represents the sorbent material as a limited set of generic surface functional groups

(e.g., strong and weak binding sites) which are responsible for adsorption. Solute partitioning data are then described by fitting batch data to an optimized set of generic surface binding sites. However, the GC approach does not allow general extrapolation of a parameterized model to other systems and fails to take advantage of previously published model parameters for idealized, single sorbent systems (Davis et al. 2004). The GC model is widely applied in sorption studies for natural materials because it requires less sorbent characterization and is less computationally challenging than the CA approach (Um et al. 2008; Hyun et al. 2009; Stoliker et al. 2011; Nair et al. 2014). The CA approach assumes that the sediment can be described as a set of known mineral components, each with specific sorption properties. The surface reactions/constants for each mineral are known from independent sorption studies or from the published literature. If surface reactions/constants for each mineral component present in the sediment can be estimated, solute adsorption by the sediment can be predicted by simply summing the adsorption behavior of individual components without the need to fit specific experimental data (i.e., calibrate) for the sediment. Since model parameters are developed for different reference minerals, they should be transferable from one field site to another (Davis et al. 2004). CA modeling is a robust scientific tool for understanding the processes controlling the partitioning and speciation of trace elements in natural systems (Groenenberg and Lofts 2014).

Understanding the surface charge characteristics of oxides and clay minerals is essential for developing mechanistic descriptions of U adsorption and/or desorption in complex natural systems. In highly weathered systems with limited organic matter, kaolinite and goethite play an important role in retarding the migration of many soil contaminants (Payne et al. 2004; Catalano and Brown Jr. 2005; Hyun et al. 2009; Bachmaf and Merkel. 2010; Zachara et al. 2013). Therefore, the objectives for this study were to identify the dominant reactive sorbent(s) controlling U(VI) partitioning for a subsurface material collected from the SRS, to develop an appropriate surface complexation model for predicting U(VI) partitioning under variable chemical conditions (i.e., pH ionic strength, etc.) based on sorption behavior in the presence of ideal reference minerals (i.e., kaolinite and goethite), and then apply the resulting SCM to the description of U(VI) partitioning in complex natural SRS materials.

Materials and methods

Materials

The SRS vadose zone material is a sandy clay loam (textural classification based on the USDA classification scheme) with a clay fraction dominated by kaolinite and

Fe-oxyhydroxides, such as goethite, typical of the Upper Coastal Plain of the southeastern USA. After collection, the material was air dried, homogenized, and passed through a 2 mm sieve before it was used in the current study (Table 1). All test solutions were prepared with ultra-pure de-ionized water (DIW; $18.2 \text{ M}\Omega \text{ cm}^{-1}$) at $25 \text{ }^\circ\text{C}$ using reagent-grade chemicals.

For batch sorption experiments, the SRS soil was dispersed and two different fractions were extracted, i.e., the clay fraction ($< 2 \text{ }\mu\text{m}$; SRS-clay) and the sand fraction ($< 2 \text{ mm}$, SRS-sand), following the procedure of (Whittig and Allardice 1986). After size fractionation, the isolates were rinsed with ultra-pure water and dried at $50 \text{ }^\circ\text{C}$ for 72 h.

Pure goethite was synthesized according to the procedure of (Schwertmann and Cornell 1991). The specific surface area of the goethite was $40.8 \pm 0.1 \text{ m}^2 \text{ g}^{-1}$, as determined by the BET methodology (Carter et al. 1986). The kaolinite standard (Georgia kaolinite, well crystallized, KGa-2), obtained from Clay Minerals Society Source Repository (Columbia, USA), was dispersed to collect the $< 2 \text{ }\mu\text{m}$ fraction for batch sorption experiments as described previously for the bulk soil. In order to represent variations in soil mineral composition, two combinations of kaolinite and goethite were tested: (1) 99% kaolinite and 1% goethite and (2) 75% kaolinite and 25% goethite.

Prior to the use in batch experiments the synthetic goethite, the kaolinite standard, the two mixtures, and the SRS-Clay fraction were suspended in 10 mM NaCl solution as stock suspension (10 g L^{-1}). Uranium stock solutions (500 mg L^{-1}) were prepared by dissolving $\text{UO}_2(\text{NO}_3)_2$ (Electron Microscopy Sciences, PA, USA) with NaCl solution.

Methods

Adsorption experiments

Sorption edge Uranium sorption edge experiments were conducted on goethite, kaolinite, the two mixtures of goethite and kaolinite, the SRS clay fraction, the SRS sand fraction, and the SRS bulk soil (Table 1). Sorption edge

experiments were performed under varied pH (3.0–10.0) in triplicate at a constant U(VI) concentration (100 mg L^{-1}) in a 10 mM NaCl solution under atmospheric $\text{CO}_2(\text{g})$ at room temperature. The zeta potential (ζ) of the equilibrated suspension was measured as described below. The sorbent concentration was 2.5 g L^{-1} for goethite, kaolinite, the goethite/kaolinite mixtures and the SRS-Clay, and $\approx 50 \text{ g L}^{-1}$ for the SRS-Sand fraction and the bulk SRS-Soil. The use of different suspension concentrations was necessary to compensate for different adsorption capacities, and to represent the natural ratio Clay/Sand, thereby allowing accurate quantification of adsorption based on residual aqueous U(VI) concentrations after equilibration with the sorptive phase.

Sample treatment Aliquots of the mineral (Goethite, Kaolinite, Mixture 1, Mixture 2, and SRS-Clay) suspensions were transferred into 50 mL polypropylene centrifuge tubes followed by addition of the U(VI) stock solution (100 mg L^{-1}). The pH was adjusted with HNO_3 or NaOH solutions to within 0.05 pH units of the target value. As a control, equivalent treatment levels were replicated in mineral-free tubes to account for any U(VI) losses in the absence of a test sorbent. The suspensions were placed on a reciprocating shaker for 72 h to equilibrate. The pH was monitored and adjusted daily to maintain the target value. All samples were equilibrated with atmospheric $\text{CO}_2(\text{g})$ by frequent exposure to air throughout equilibration. The failure to achieve full equilibration with CO_2 can impact the U(VI)-carbonate speciation, which is important in accurately describing U(VI) partitioning. Prior to analysis, the solid and solution phases were separated by centrifugation (Sorvall RC 5B, 1000 rpm, 20 min), followed by filtration of the supernatant (with $< 0.22 \text{ }\mu\text{m}$ pore size PES filters), with the first 0.5 mL of filtrate discarded. The filtrate was acidified (2% HNO_3) for preservation and analyzed for U by inductively coupled plasma-mass spectrometry (ICP-MS, NexION 300X, PerkinElmer, Akron, Ohio 44311) using the protocols outlined in EPA Method 6020B (USEPA 2014).

The percentage of U(VI) sorbed was calculated from the difference between the initial and final U(VI) concentrations as follows:

$$\text{Sorption (\%)} = \left(\frac{C_i - C_f}{C_i} \right) * 100$$

where C_i and C_f are the U concentration in the initial and final solutions, respectively. Control experiments indicated that U(VI) adsorption by the vial walls was negligible under all test conditions.

Electrochemical measurements

Zeta potentials of equilibrated suspensions from the Sorption Edge experiments were determined from their

Table 1 Characteristics of the SRS soil

Soil	(SRS soil)
PSD	
% Sand	68.3
% Silt	4.1
% Clay	27.7
pH _{DIW}	4.56 ± 0.9
CEC (cmol kg^{-1})	1.01 ± 0.17
CBD ext. Fe (mg g^{-1})	12.82 ± 0.28
Clay mineralogy	Kaol, Goe, Ill

electrophoretic mobilities (EM) according to the Smoluchowski equation (Sze et al. 2003). The Phase Analysis Light Scattering (PALS) method (ZetaPlus Analyzer, Brookhaven Instruments Corp., Holtsville, NY) was used to measure EMs of particles in the background solution. For PALS measurement, 50 μL of each suspension were transferred to an EM tube and then diluted with 4 mL of clear supernatant (i.e., filtered) from the same batch treatment. The electrode assembly, pre-equilibrated in 10 mM NaCl for 24 h before each use, was inserted into the vial and fully submerged by the suspensions. All measurements were run 10 times at 25 °C.

Modeling

The geochemical computer code PHREEQC-2 (Parkhurst and Appelo 1999) was used for calculation and modeling of U(VI) speciation and adsorption. Electrostatic SCMs (containing electrical double layer correction terms in the mass law for adsorption reactions) for goethite and kaolinite were selected/modified from existing literature (Dong and Wan 2014) to describe our experimental data for U(VI) adsorption onto reference minerals, i.e., goethite and kaolinite. The adsorption data obtained with the standard minerals (Goethite, Kaolinite, and quartz) was used to calculate the sorption constants and to test the goodness of fit for any

proposed reactions. The nonlinear, least-squares optimization program PEST (Doherty 2010) was used to adjust the values of unknown surface complex formation constants in a chemical equilibrium model to yield the best fit of the reaction scheme to the experimental data (Fig. 1).

Using the calculated constants based on experimental data, a CA model was then developed to predict U(VI) adsorption behavior for the SRS bulk soil, with goethite, kaolinite, and quartz as the adsorbing component minerals (Fig. 1).

Results and discussion

Zeta potential measurement

Figure 2 presents the electrophoretic mobilities as a function of pH obtained upon adsorption of U(VI) onto goethite, kaolinite, the two mixtures, and the SRS clay fraction. The Point of Zero Charge (pH_{PZC}) is the pH where crossover between negative and positive electrophoretic mobilities occurs. For the sorptive minerals, the pH_{PZC} is approximately 8 for goethite (Fig. 2a), pH 4.5 for kaolinite (Fig. 2b), pH 4.5 for clay Mixture 1 (Fig. 2c), pH 5.5 for Mixture 2 (Fig. 2d), and 5.5 for the SRS clay fraction (Fig. 2e). The pH_{PZC} for goethite and kaolinite is in agreement with values commonly

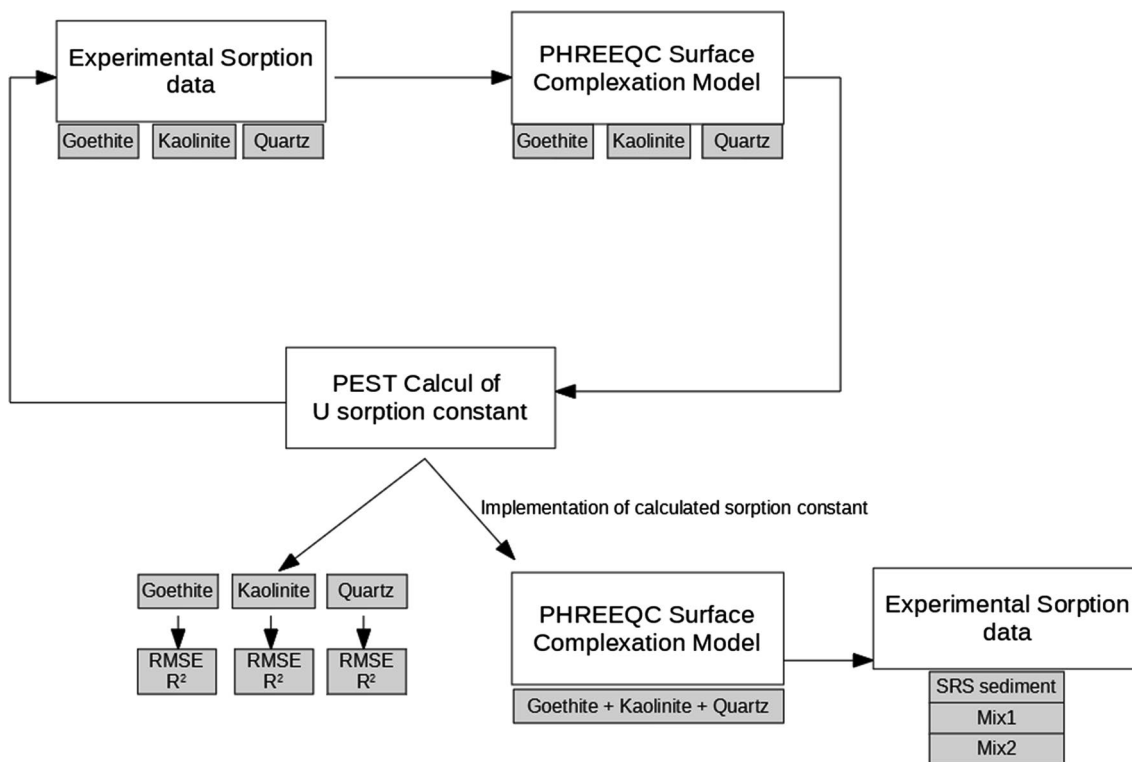


Fig. 1 Flowchart of the modeling processes

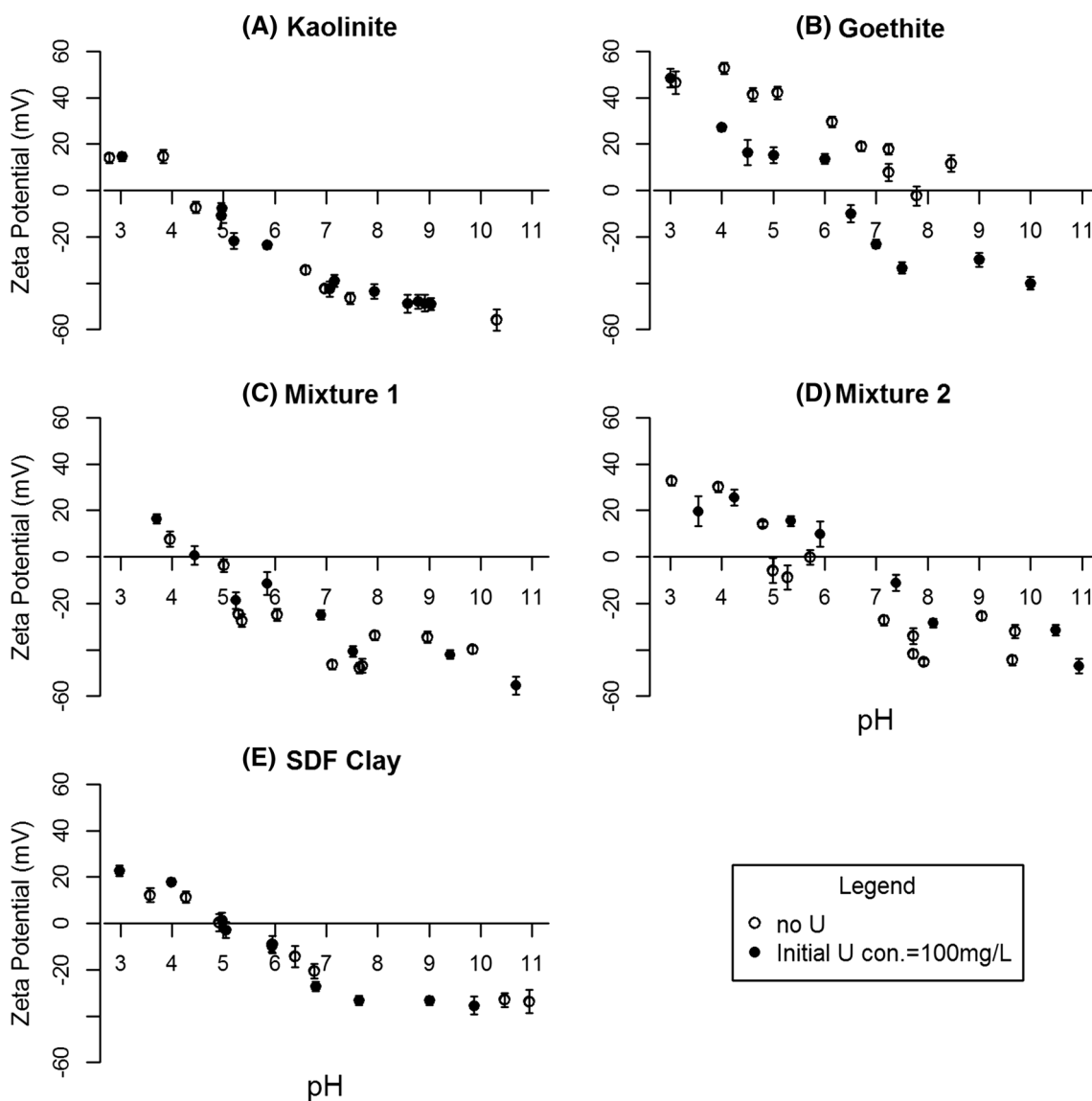


Fig. 2 Zeta potential of 2.5 g L⁻¹ Goethite, Kaolinite, Mix1, Mix2, and SRS clay fraction as a function of pH

reported in the literature (Goldberg et al. 1996; Celi et al. 2001).

The pH_{PZC} of Mixture 1 and kaolinite is essentially identical, with goethite showing little discernible impact on the surface charge of the suspension at such low mass concentrations. In contrast, Mixture 2 has a pH_{PZC} of 5.5, a full pH unit higher than observed for pure kaolinite suspension. Thus, adding goethite to the mixture shifts the pH_{PZC} to higher values, closer to the pH_{PZC} of the Fe-oxyhydroxide. The SRS-clay fraction has a pH_{PZC} similar to Mixture 2.

In the presence of U(VI), the zeta potential of the goethite suspension was lower at a given pH, with the pH_{PZC} shifting from pH 8–6. A shift in the pH_{PZC} is characteristic of specific ion adsorption behavior with the sorbed species altering the surface properties of the sorbent (Goldberg et al. 1996;

Liu et al. 2008). The significant shift of pH_{PZC} of goethite to a lower pH in the presence of U(VI) (Fig. 2) suggests that U(VI) forms inner-sphere complexes at the goethite surface. A similar shift of pH_{PZC} is readily apparent for the mixture treatment containing the higher goethite to kaolinite ratio (i.e., Mixture 2).

In contrast, the observed zeta potentials for kaolinite, Mixture 1 (99% kaolinite by mass), and the SRS clay fraction were generally insensitive to the presence of U(VI). However, the absence of a shift in pH_{PZC} in the presence of an ionic sorbing species cannot be used to infer a strictly outer-sphere adsorption mechanism since inner-sphere surface complex formation is not necessarily accompanied by a change in the mineral surface charge (Goldberg and Johnston 2001).

Uranium aqueous speciation

Aqueous speciation was computed for the solution with a total U (ΣU) concentration of 100 mg L^{-1} in a background

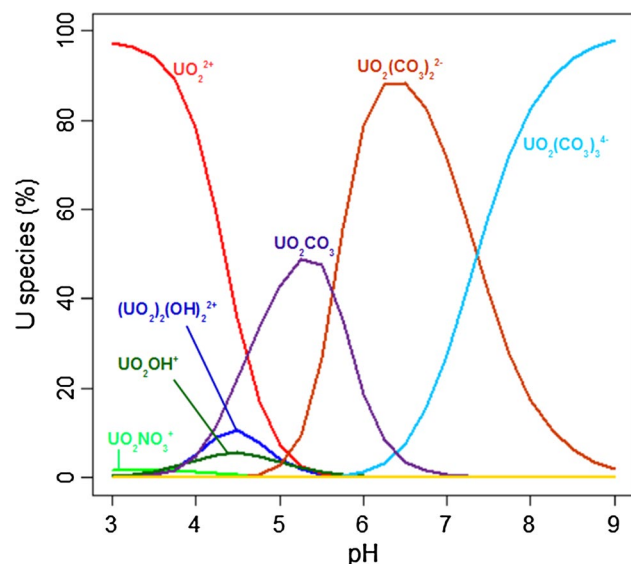


Fig. 3 Uranyl aqueous speciation in 10 mM NaCl, $\Sigma U = 100 \text{ mg L}^{-1}$

electrolyte of 10 mM NaCl equilibrated with atmosphere (i.e., partial pressure of $\approx 10^{-3.5}$ atm for P_{CO_2}). The distribution of aqueous species was calculated with the geochemical code PHREEQC-2 (Parkhurst and Appelo 1999) using the wateq.4f database. Aqueous phase U(VI) speciation as a function of pH is presented in Fig. 3. Under these conditions, U(VI) interaction with dissolved inorganic carbon plays a major role in determining aqueous phase U(VI) speciation. Free uranyl UO_2^{2+} is the dominant species in the acidic pH range up to 5 (Arnold et al. 2001; Guo et al. 2009; Bachmajer and Merkel 2010). With increasing pH, U(VI) speciation is dominated by U hydrolysis products and carbonate species.

U(VI) adsorption data

U(VI) adsorption was calculated from the difference of aqueous phase U(VI) before and after equilibration. To directly compare the adsorption capacity of various test sorbents, the experimental data are presented in terms of the percentage of the total U(VI) added (Figs. 4a, 5a).

The adsorption data of U(VI) onto quartz, kaolinite, and goethite are compared in Fig. 4a. The data shows that the quartz surface has a weaker adsorption capacity than goethite or kaolinite at pH values < 6 and > 7 . At $\text{pH} \approx 5$, for example, 88% of U(VI) was sorbed by kaolinite and 72% by

Fig. 4 Comparison batch U(VI) sorption data and the SCM model results for the SRS-clay fraction (a), kaolinite (b), goethite (c), and quartz (d). Experimental conditions: $\Sigma U = 100 \text{ mg L}^{-1}$, $P_{\text{CO}_2} 10^{-3.5} \text{ hPa}$, 25°C , ionic strength 0.01 M NaCl. The black solid lines are the overall model fits and the dotted lines with numbers are the fitted distributions specific surface: (3) $(\text{FeOH})_2\text{UO}_2^+$ from the equation 3 of Table 2; (4) $(\text{FeOH})_2\text{UO}_2\text{CO}_3^-$; (11) FeOUO_2^+ ; (14) $(\text{KsOH})_2\text{UO}_2^+$; (15) $(\text{KsOH})_2\text{UO}_2\text{CO}_3^-$; (20) $(\text{QOH})_2\text{UO}_2^{+2}$; and (21) $(\text{QOH})_2\text{UO}_2\text{CO}_3$

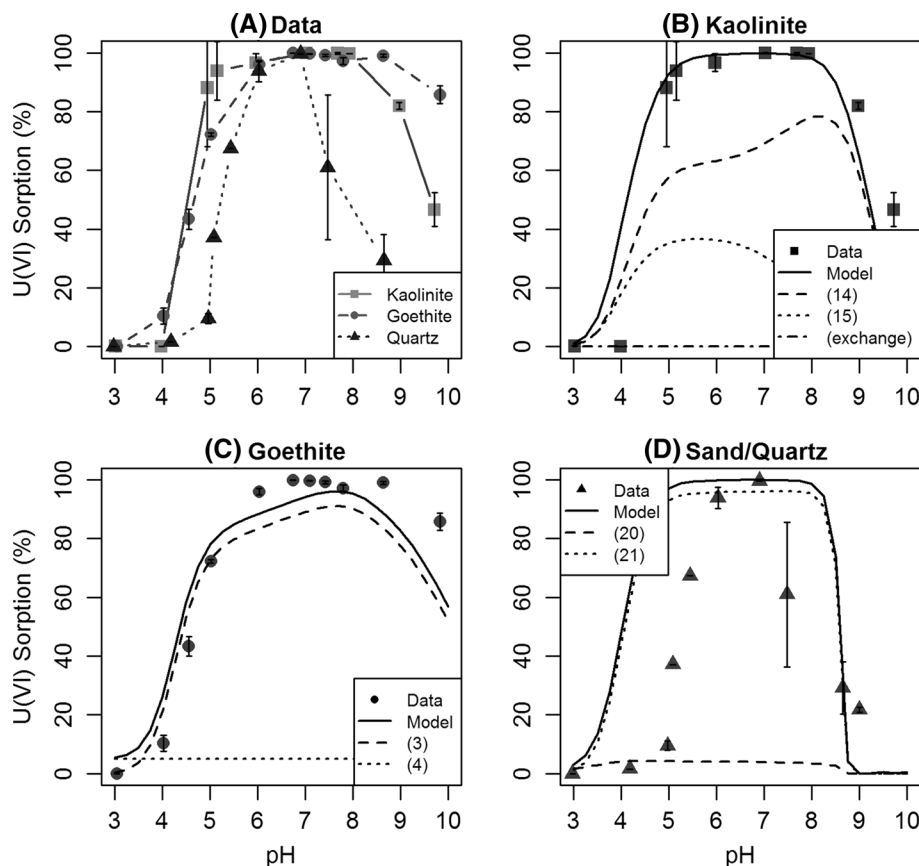
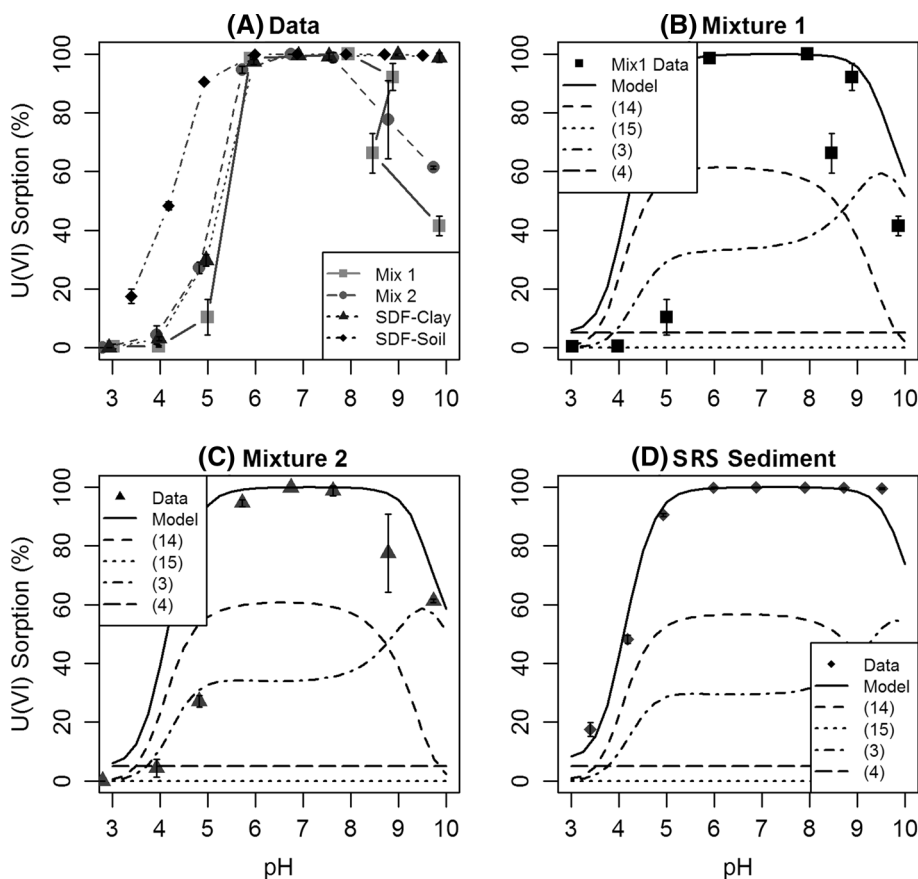


Fig. 5 Comparison of batch U(VI) sorption data and the SCM modeling results for the SRS clay fraction (a), Mix 1 (b), Mix 2 (c), and the SRS bulk soil (d). Experimental conditions: $\Sigma U = 100 \text{ mg L}^{-1}$, $P_{\text{CO}_2} = 10^{-3.5} \text{ kPa}$, $25 \text{ }^\circ\text{C}$, ionic strength 0.01 M NaCl . The black solid lines are the overall model fits and the dotted lines with numbers are the fitted distributions specific surface: (3) $(\text{FeOH})_2\text{UO}_2^+$ from the equation 3 of Table 2; (4) $(\text{FeOH})_2\text{UO}_2\text{CO}_3^-$; (11) FeOUO_2^+ ; (14) $(\text{KsOH})_2\text{UO}_2^+$; (15) $(\text{KsOH})_2\text{UO}_2\text{CO}_3^-$; (20) $(\text{QOH})_2\text{UO}_2^{+2}$; and (21) $(\text{QOH})_2\text{UO}_2\text{CO}_3$



by goethite, while only 9.5% was sorbed by quartz. At low pH ($\text{pH} < 6$), kaolinite is the most effective sorbent. This observation can be explained by the amphoteric behavior of the two more sorptive minerals, i.e., goethite and kaolinite. As shown in Fig. 2, the pH_{PZC} of kaolinite occurs at $\text{pH} \approx 4.5$, displaying a net negative surface charge at $\text{pH} > 4.5$ such that adsorption of the positively charged UO_2^{2+} species is enhanced by electrostatic attraction. In contrast, goethite has the pH_{PZC} at $\text{pH} \approx 8$. Thus, goethite surfaces are net positively charged at $\text{pH} < 8$, which can hinder UO_2^{2+} sorption due to electrostatic repulsion.

In the literature, strong U(VI) adsorption at $\text{pH} < 4$ onto kaolinite has been attributed to the contribution of cation exchange sites (i.e., limited isomorphous substitution in kaolinite and/or the presence of clay mineral impurities) at low ionic strength (Dong et al. 2012). However, in the current experiment such behavior was not observed. As shown by (Bachmaf and Merkel 2010), our kaolinite displayed very limited U(VI) sorption capacity at low pH (< 4) and a greater adsorption than goethite or quartz in the pH range of 5–8. (Bachmaf and Merkel 2010) also reported a minor ionic strength dependency for U(VI) adsorption by kaolinite at $\text{pH} > 6$. Therefore, we can assume that under the present conditions, the importance of cation exchange

capacity in controlling U(VI) sorption associated with kaolinite at low pH is negligible.

The strong adsorption by goethite at pH values above 6 is consistent with previous observations in the literature where iron (oxy)hydroxides, such as amorphous iron hydroxide, i.e., ferrihydrite, and crystalline oxyhydroxides such as goethite, have been identified as major adsorptive surfaces for U(VI) (Barnett et al. 2000; Sherman et al. 2008; Um et al. 2008; Dong et al. 2012).

The adsorption capacity of clay Mixture 1, Mixture 2, the SRS clay fraction, and the SRS bulk soil is compared in Fig. 5a. Similar U(VI) adsorption for all four samples is observed at $\text{pH} < 7$, while adsorption is stronger to the SRS clay fraction and SRS bulk soil than the two mixtures of goethite and kaolinite for higher pH (alkaline conditions). Adsorption at $\text{pH} < 7$ (acidic conditions) can be attributed to the goethite and kaolinite, while other trace minerals may be responsible for the higher than expected sorption of U(VI) at pH values above 7. As noted above, quartz in this soil displays limited U(VI) adsorption between pH 6 and 7 and thus is unlikely to be responsible for the strong U(VI) sorption observed under alkaline pH conditions. In addition, the sorption curves for the SRS-Clay fraction and the bulk SRS-Soil are quite similar, again suggesting a limited role for quartz in

U(VI) sorption under alkaline conditions. Characterization of the mineralogy for the < 2 μm fraction showed a small amount of illite was present in the SRS sediment (Table 1). (Geckeis et al. 2013) have shown that in a pure NaCl system, there is a high uptake of U(VI) sorbed by illite at high pH (i.e., between pH 6.5 and 11).

Surface complexation modeling

To illustrate the relative contribution of individual minerals and specific surface species to the overall adsorption of U(VI), the experimental data and modeling results are presented in terms of percentages (Fig. 4).

A large variety of SCMs have been applied to U(VI) sorption on Fe oxyhydroxides, e.g., goethite: first, the use of ferrihydrite as a model surface (Waite et al. 1994; Fox et al. 2006; Mahoney et al. 2009) and monodentate sorption complexes (Missana et al. 2003) has been widely used in order to describe U(VI) sorption on goethite. However, goethite zeta potentials in presence of U(VI) display a shift in the pH_{ZPC} from pH 8–6, indicating the formation of inner-sphere U(VI) surface complexes at the goethite surface that increases the net positive surface character at a given pH. In the present study, U(VI) sorption is attributed to the formation of two bidentate surface complexes at goethite edge sites, consistent with the multisite SCM developed by (Sherman et al. 2008) to describe U(VI) sorption by goethite based on their extended X-ray adsorption fine structure (EXAFS) spectra data. A direct application of the (Sherman et al. 2008) model was used by (Dong et al. 2012) to describe sorption behavior for similar SRS soil materials.

Earlier modeling attempts at describing U(VI) sorption by kaolinite have involved various assumptions. (Payne et al. 2004) postulated that U(VI) sorption by kaolinite occurs at both aluminol (AlOH) sites associated with kaolinite and titanol (TiOH) sites attributed to anatase impurities identified by transmission electron microscopy equipped with energy-dispersive X-ray spectrometry (TEM/EDS), with U(VI) preferentially bound to the anatase impurities. However, application of these two mineral surfaces tended to over predict the amount of U(VI) adsorbed under low pH conditions (i.e., $\text{pH} < 5$). Monodentate surface complexes have also been proposed via reactions of clay edge surface sites with major U(VI) species in aqueous phase (Borovec 1981; Turner and Sassman 1996; Pabalan and Turner 1996; Kremleva et al. 2008). In our model, U(VI) sorption by kaolinite (Georgia kaolinite, KGa-2) is through the formation of two bidentate surface complexes at mineral edge sites, an approach adapted from (Dong et al. 2012). Their assumption was supported by spectroscopic evidence that revealed at low pH and low ionic strength, U(VI) sorption behavior was dominated by fixed-charge sites, while at high pH bidentate inner-sphere surface AlOH and SiOH edge sites were responsible for sorption (Pabalan and Turner

1996; Kowal-Fouchard et al. 2004), with uranyl-carbonate ternary surface complexes present in systems equilibrated with atmospheric CO_2 (Catalano and Brown Jr. 2005; Sherman et al. 2008). Those assumptions were also supported by (Krepelova et al. 2007). The KsOH sites (Table 2) represent both silanol (SiOH) and aluminol (AlOH) sites on kaolinite surfaces.

The U(VI) sorption onto quartz has been studied extensively (Turner and Sassman 1996; Prikryl et al. 2001; Davis et al. 2004; Nair et al. 2014). Dong and Wan (2014) proposed an adsorption for U(VI) based on inner-sphere bidentate complexes and the formation of ternary uranyl-carbonate surface complexes.

Few studies have evaluated U(VI) sorption by illite. (Bradbury and Baeyens 2009) used linear free energy relationships and a two-site protolysis non-electrostatic surface complexation and cation exchange model to describe U(VI) sorption to illite, an approach adopted in the current study. In contrast to (Dong and Wan 2014) and (Dong et al. 2012), the direct application of those model parameters without any adjustment for differences in reactive surface area of the relevant sorbent materials was not effective. As widely noted in the literature (Sverjensky 2003; Davis et al. 2004), surface complexation constants are dependent on the surface area and reactive site density of the sorbent in question.

The equilibrium constants for the acid–base surface reactions of goethite, kaolinite, and quartz sites (Eq. 1, 2, 12, 13, 18, and 19 in Table 2) are based on values reported in (Dong and Wan 2014), while the constants for the acid–base surface reactions of illite (Eq. 24 and 25 in Table 2) were taken from (Bradbury and Baeyens 2009). The nonlinear least-squares parameters estimation program PEST 6.05 (Doherty 2010) in conjunction with PHREEQC-2 (Parkhurst and Appelo 1999) was used to determine the equilibrium constants for the other surface reactions given in Table 2. PEST has the advantage over FIQTEL (Westall 1985) in that activity coefficients can be calculated according to either extended Wateq Debye–Hückel or SIT (specific ion interaction theory) and provides users with statistical information on the uncertainty of the estimation (Bachmaf and Merkel 2010). A discussion of the methodology for estimating sorption constants from experimental data using the two computer programs, i.e., PEST and PHREEQC, is provided by (Bachmaf and Merkel 2011).

The goodness of fit for ability of the model to describe experimental data were quantified by the root mean squared error (RMSE) as well as the correlation coefficient (as calculated by PEST) (Table 3). The RMSE is calculated as:

$$\text{RMSE} = \left[\frac{1}{n_d - n_p} \sum_{i=1}^{n_d} (\% \text{Rem} - \% \text{Rem}^*)^2 \right]^{1/2}$$

Table 2 Surface reactions and parameters used in the model calculations. If not indicated by Dong and Wan (2014) or Bradbury and Baeyens (2009), data were calculated with PEST and PHREEQC-2

		Log_K	References
<i>Surface reaction on goethite</i>			
(1)	$\text{FeOH}^{-0.5} = \text{FeOH}^{-0.5}$	0	Dong and Wan (2014)
(2)	$\text{FeOH}^{-0.5} + \text{H}^+ = \text{FeOH}_2^{+0.5}$	9.18	Dong and Wan (2014)
(3)	$2\text{FeOH}^{-0.5} + \text{UO}_2^{+2} = (\text{FeOH})_2\text{UO}_2^+$	13.0860	Adjusted
(4)	$\text{CO}_2 + 2\text{FeOH}^{-0.5} + \text{H}_2\text{O} + \text{UO}_2^{+2} = (\text{FeOH})_2\text{UO}_2\text{CO}_3^- + 2\text{H}^+$	10.00	Adjusted
(5)	$\text{CO}_2 + 2\text{FeOH}^{-0.5} = (\text{FeO})_2\text{CO}^- + \text{H}_2\text{O}$	5.93	Dong and Wan (2014)
(6)	$\text{CO}_2 + \text{FeOH}^{-0.5} + \text{Na}^+ = \text{FeOCO}_2\text{Na}^{-0.5} + \text{H}^+$	- 3.02	Dong and Wan (2014)
(7)	$\text{Al}^{+3} + \text{FeOH}^{-0.5} + \text{H}_2\text{O} = \text{FeOHAl}(\text{OH})^{+1.5} + \text{H}^+$	7	Dong and Wan (2014)
(8)	$\text{Al}^{+3} + \text{FeOH}^{-0.5} + 2\text{H}_2\text{O} = \text{FeOHAl}(\text{OH})_2^{+0.5} + 2\text{H}^+$	- 0.61	Dong and Wan (2014)
<i>Surface reaction on kaolinite</i>			
(12)	$\text{KsOH}^{-0.5} = \text{KsOH}^{-0.5}$	0	Dong and Wan (2014)
(13)	$\text{KsOH}^{-0.5} + \text{H}^+ = \text{KsOH}_2^{+0.5}$	4.9	Dong and Wan (2014)
(14)	$2\text{KsOH}^{-0.5} + \text{UO}_2^{+2} = (\text{KsOH})_2\text{UO}_2^+$	5.36478	Adjusted
(15)	$2\text{KsOH}^{-0.5} + \text{UO}_2^{+2} + \text{H}_2\text{CO}_3 = (\text{KsOH})_2\text{UO}_2\text{CO}_3^- + 2\text{H}^+$	- 0.394846	Adjusted
(16)	$\text{KsOH}^{-0.5} + \text{Na}^+ = \text{KsOHNa}^{+0.5}$	- 2.1	Dong and Wan (2014)
(17)	$\text{KsOH}^{-0.5} + \text{H}^+ + \text{NO}_3^- = \text{KsOH}_2\text{NO}_3^{-0.5}$	4.9	Dong and Wan (2014)
<i>Surface reaction on quartz</i>			
(18)	$\text{QOH} = \text{QOH}$	0	Dong and Wan (2014)
(19)	$\text{QOH} = \text{QO}^- + \text{H}^+$	- 7.20	Dong and Wan (2014)
(20)	$2\text{QOH} + \text{UO}_2^{+2} = (\text{QOH})_2\text{UO}_2^{+2}$	5.12	Adjusted
(21)	$2\text{QOH} + \text{UO}_2^{+2} + \text{CO}_2 + \text{H}_2\text{O} = (\text{QOH})_2\text{UO}_2\text{CO}_3 + 2\text{H}^+$	0.26	Adjusted
(22)	$\text{QOH} + \text{Al}^{+3} + 3\text{H}_2\text{O} = \text{QOHAl}(\text{OH})_3 + 3\text{H}^+$	- 9.00	Dong and Wan (2014)
<i>Surface reaction on illite</i>			
(23)	$\text{IllOH} = \text{IllOH}$	0	
(24)	$\text{IllOH} + \text{H}^+ = \text{IllOH}_2^+$	4.0	Bradbury and Baeyens (2009)
(25)	$\text{IllOH} = \text{IllO}^- + \text{H}^+$	- 6.2	Bradbury and Baeyens (2009)
(26)	$\text{IllOH} + \text{UO}_2^{+2} + \text{H}_2\text{O} = \text{IllOUO}_2\text{OH}^0 + 2\text{H}^+$	- 3.5	Bradbury and Baeyens (2009)
(27)	$\text{IllOH} + \text{UO}_2^{+2} + 2\text{H}_2\text{O} = \text{IllOUO}_2(\text{OH})_2 + 3\text{H}^+$	- 10.6	Bradbury and Baeyens (2009)

Goethite site = FeOH, kaolinite site = KsOH, quartz site = QOH, ill = illite site

Table 3 Model parameters for reference minerals

	Kaolinite	Goethite	Quartz	Mix 1	Mix 2	SRS-clay fraction (not presented)	SRS-soil
Sites density (mol nm ⁻²)	2.161 0 ^{-3a}	3.090 10 ^{-3a}	1.470 10 ^{-3a}				
Surface area (m ² g ⁻¹)	21.5 ^b	40.775	0.2 ^c				
Ionic strength	0.01 M NaCl						
PCO ₂	10 ^{-3.5} atm						
Number of data points	36	31	25	30	30	27	23
Correlation coefficient	0.93	0.96	0.69	0.80	0.87	0.75	0.95
RMSE	18.3	12.0	40.5	31.1	24.2	35.0	10.2

^aAdjusted

^bFrom Bachmaf and Merkel (2010)

^cFrom Dong and Wan (2014)

where n_d is the number of data points (Table 3), n_p is the number of adjustable parameters (zero when used in a purely predictive manner), % Rem is the percentage of U(VI) sorbed in the laboratory experiments, and % Rem* is the percentage of U(VI) sorbed as predicted by the model. The RMSE is a measure of the error between the predicted and the measured values expressed in dimensionless form (e.g., the smaller the RMSE, the better is the fit of the model to the data).

The correlation coefficient R is calculated by PEST as follows:

$$R = \frac{\sum (w_i c_i - m)(w_i c_{0i} - m_0)}{\left[\left[\sum (w_i c_i - m)(w_i c_i - m) \sum (w_i c_{0i} - m_0)(w_i c_{0i} - m_0) \right] \right]^{1/2}}$$

where c_i is the i 'th observation value, c_{0i} is the model-generated counterpart to the i 'th observation value, m is the mean value of weighted observations, m_0 is the mean of weighted model-generated counterparts to the observations, and w_i is the weight associated with the i 'th observation (or "rotated observation" if a covariance matrix is used to specify observation uncertainty instead of individual observation weights). Generally, R should be above 0.9 for the fit between model outputs and observations to be considered as acceptable (Hill 1998).

The data presented in Fig. 4 indicate that the model predicts the major trends of U(VI) sorption with respect to pH for goethite and kaolinite. In contrast, the model over predicted U(VI) sorption on quartz for a pH range above and below 7.

The root mean square errors (RMSE) were 18.3, 12.0, and 40.5 for goethite, kaolinite, and quartz, respectively.

For goethite, Fig. 4c indicates that surface species $(\text{FeOH})_2\text{UO}_2^+$ dominates at all pHs, while the $(\text{FeOH})_2\text{UO}_2\text{CO}_3^-$ species is rather minor for all pHs.

For kaolinite, cation exchange was not included in the model because we experimentally observed little to no U(VI) adsorption at low pH, and calculations indicated that cation exchange was negligible ($< 0.01\%$) under our experimental conditions. Figure 4b shows that one type of surface site with two bidentate surface complexes can reasonably predict U(VI) adsorption behavior for kaolinite. The bidentate $(\text{KsOH})_2\text{UO}_2^+$ is responsible for 60–77% of the U(VI) sorption on kaolinite between pH 5 and 8.5, while the uranyl-carbonate ternary surface $(\text{KsOH})_2\text{UO}_2\text{CO}_3^-$ is responsible for 40 to 33%.

Model simulations for the goethite and kaolinite mixtures were conducted using the appropriate equations presented in Table 2, with the reactive site density and the surface area values provided in Table 3. Figure 5b, c presents the simulated data for Mixture 1 and Mixture 2, respectively. The RMSE values are 31.14 and 21.27 for

Mixture 1 and Mixture 2, respectively, showing that the model is in good agreement with the experimental data. This suggests that the mixtures of goethite and kaolinite can be reasonably described based on the relative fractions of the two sorbent materials. For $\text{pH} < 9$, the kaolinite is the major surface responsible for the uptake of U (61% for $(\text{KsOH})_2\text{UO}_2^+$ of kaolinite and 33% for $(\text{GOH})_2\text{UO}_2^+$ of goethite), while it is the goethite for a $\text{pH} > 9$.

The SRS sediment (SRS-soil) is mainly composed of goethite, kaolinite, and quartz, which suggests that the CA approach can be an effective method for simulating U(VI) sorption behavior. Figure 5d indicates that the modeling of the data based on goethite, kaolinite, and quartz can predict the behavior of U(VI) in the natural sediment for pH values from 3 to 9. Based on the fitted data, the kaolinite is responsible for 56% of U(VI) sorption, the goethite for 30%, and quartz represents less than 1%. However, the model under predicts U(VI) sorption for $\text{pH} > 9$. As discussed earlier, the clay mineralogy consists of a small amount of illite that may be responsible for U(VI) sorption at high pH. However, including equations 26 and 27 in the model does not fully address this discrepancy. A more reasonable explanation is that the experimental batches may not have been in full equilibrium with the atmospheric $\text{CO}_2(\text{g})$, which has implications to U(VI)-carbonate speciation, leading to higher than expected sorption at higher pH.

Conclusions

Experimental and modeled data derived from this study indicate that the use of the PEST code together with PHREEQC is an extremely powerful tool to estimate experimental equilibrium constants. These results also demonstrate the significant and sometimes unexpected effects that pH and aqueous phase speciation can have on U(VI) adsorption, that these effects are sometimes not observed in experiments at constant $\text{CO}_2(\text{g})$ partial pressure, and the need to consider these effects when modeling U(VI) mobility in the natural environment. Geochemical modeling and laboratory experiments on water–rock–gas interactions improve understanding of mineral alteration processes and can be applied to a variety of applications (i.e. $\text{CO}_2(\text{g})$ storage, groundwater modeling...).

Model discrepancies observed at low pH for mixtures of kaolinite and goethite may be due to the combined mineral interactions that restrict access to sorption sites on the kaolinite surface. Nonetheless, the results indicate that a simple CA approach may yield useful predictions of contaminant sorption in mixed mineral assemblages, provided that robust SCMs are available for the appropriate reactive system components. However, it should be noted that the relatively rapid nature of the batch sorption experiments may underestimate

the effects of aging processes and the influence of slower-forming coatings in potentially blocking metal adsorption sites on natural soils and sediments. Before SCMs can be applied to natural systems, several other hurdles remain, including the development of methods to correctly assess the dominant sorption phases and their reactive surface areas within complex soils and sediments.

Acknowledgements This study was supported by the US Department of Energy under Award Numbers DEFC09-07SR22506 to the University of Georgia Research Foundation.

References

- Arnold T, Zorn T, Bernhard G, Nitsche H (1998) Sorption of uranium(VI) onto phyllite. *Chem Geol* 151:129–141. [https://doi.org/10.1016/S0009-2541\(98\)00075-8](https://doi.org/10.1016/S0009-2541(98)00075-8)
- Arnold T, Zorn T, Zänker H et al (2001) Sorption behavior of U(VI) on phyllite: experiments and modeling. *J Contam Hydrol* 47:219–231. [https://doi.org/10.1016/S0169-7722\(00\)00151-0](https://doi.org/10.1016/S0169-7722(00)00151-0)
- Bachmaf S, Merkel BJ (2010) Sorption of uranium(VI) at the clay mineral–water interface. *Environ Earth Sci* 63:925–934. <https://doi.org/10.1007/s12665-010-0761-6>
- Bachmaf S, Merkel BJ (2011) Estimating water chemistry parameters from experimental data using PEST with PHREEQC. *FOG Freib Online Geosci* 28:1–18
- Barnett MO, Jardine PM, Brooks SC, Selim HM (2000) Adsorption and transport of uranium(VI) in subsurface media. *Soil Sci Soc Am J* 64:908. <https://doi.org/10.2136/sssaj2000.643908x>
- Borovec Z (1981) The adsorption of uranyl species by fine clay. *Chem Geol* 32:45–58. [https://doi.org/10.1016/0009-2541\(81\)90127-3](https://doi.org/10.1016/0009-2541(81)90127-3)
- Bradbury MH, Baeyens B (2009) Sorption modelling on illite. Part II: actinide sorption and linear free energy relationships. *Geochim Cosmochim Acta* 73:1004–1013. <https://doi.org/10.1016/j.gca.2008.11.016>
- Carter DL, Mortland MM, Kemper WD (1986) Specific surface. In: Klute A (ed) *Methods of soil analysis, part 1. Physical and mineralogical methods*, 2nd edn. ASA, Madison, pp 413–423
- Catalano JG, Brown GE Jr (2005) Uranyl adsorption onto montmorillonite: evaluation of binding sites and carbonate complexation. *Geochim Cosmochim Acta* 69:2995–3005. <https://doi.org/10.1016/j.gca.2005.01.025>
- Celi L, Presta M, Ajmore-Marsan F, Barberis E (2001) Effects of pH and electrolytes on inositol hexaphosphate interaction with goethite. *Soil Sci Soc Am J* 65:753. <https://doi.org/10.2136/sssaj2001.653753x>
- Chang H, Buettner SW, Seaman JC et al (2014) Uranium immobilization in an iron-rich rhizosphere of a native wetland plant from the savannah river site under reducing conditions. *Environ Sci Technol* 48:9270–9278. <https://doi.org/10.1021/es5015136>
- Cheng T, Barnett MO, Roden EE, Zhuang J (2004) Effects of phosphate on uranium(VI) adsorption to goethite-coated sand. *Environ Sci Technol* 38:6059–6065
- Davis JA (2003) Application of surface complexation modeling to describe uranium (VI) adsorption and retardation at the uranium mill tailings site at Naturita, Colorado. Division of Systems Analysis and Regulatory Effectiveness, Office of Nuclear Regulatory Research, U.S. Nuclear Regulatory Commission, Washington
- Davis JA, Coston JA, Kent DB, Fuller CC (1998) Application of the surface complexation concept to complex mineral assemblages. *Environ Sci Technol* 32:2820–2828. <https://doi.org/10.1021/es980312q>
- Davis JA, Meece DE, Kohler M, Curtis GP (2004) Approaches to surface complexation modeling of Uranium(VI) adsorption on aquifer sediments I. *Geochim Cosmochim Acta* 68:3621–3641. <https://doi.org/10.1016/j.gca.2004.03.003>
- Doherty J (2010) Methodologies and software for PEST-based model predictive uncertainty analysis. PEST user manual
- Dong W, Wan J (2014) Additive surface complexation modeling of uranium(VI) adsorption onto quartz-sand dominated sediments. *Environ Sci Technol* 48:6569–6577. <https://doi.org/10.1021/es501782g>
- Dong W, Tokunaga TK, Davis JA, Wan J (2012) Uranium(VI) adsorption and surface complexation modeling onto background sediments from the F-area Savannah River Site. *Environ Sci Technol* 46:1565–1571. <https://doi.org/10.1021/es2036256>
- Fox PM, Davis JA, Zachara JM (2006) The effect of calcium on aqueous uranium(VI) speciation and adsorption to ferrihydrite and quartz. *Geochim Cosmochim Acta* 70:1379–1387. <https://doi.org/10.1016/j.gca.2005.11.027>
- Geckeis H, Altmaier M, Fanghaenel S (2013) Annual report 2013/ Institute for Nuclear Waste Disposal. KIT Scientific Publishing, Karlsruhe
- Goldberg S, Johnston CT (2001) Mechanisms of arsenic adsorption on amorphous oxides evaluated using macroscopic measurements, vibrational spectroscopy, and surface complexation modeling. *J Colloid Interface Sci* 234:204–216. <https://doi.org/10.1006/jcis.2000.7295>
- Goldberg S, Forster HS, Godfrey CL (1996) Molybdenum adsorption on oxides, clay minerals, and soils. *Soil Sci Soc Am J* 60:425. <https://doi.org/10.2136/sssaj1996.03615995006000020013x>
- Groenenberg JE, Lofts S (2014) The use of assemblage models to describe trace element partitioning, speciation, and fate: a review: review assemblage models. *Environ Toxicol Chem* 33:2181–2196. <https://doi.org/10.1002/etc.2642>
- Guo Z, Li Y, Wu W (2009) Sorption of U(VI) on goethite: effects of pH, ionic strength, phosphate, carbonate and fulvic acid. *Appl Radiat Isot* 67:996–1000. <https://doi.org/10.1016/j.apradiso.2009.02.001>
- Hill MC (1998) Methods and guidelines for effective model calibration. Water-Resources Investigations Report, U. S. Geological Survey, Denver, CO
- Hyun SP, Fox PM, Davis JA et al (2009) Surface complexation modeling of U(VI) adsorption by aquifer sediments from a former mill tailings site at Rifle, Colorado. *Environ Sci Technol* 43:9368–9373. <https://doi.org/10.1021/es902164n>
- Jerden JL Jr, Sinha AK, Zelazny L (2003) Natural immobilization of uranium by phosphate mineralization in an oxidizing saprolite–soil profile: chemical weathering of the Coles Hill uranium deposit, Virginia. *Chem Geol* 199:129–157. [https://doi.org/10.1016/S0009-2541\(03\)00080-9](https://doi.org/10.1016/S0009-2541(03)00080-9)
- Kowal-Fouchard A, Drot R, Simoni E, Ehrhardt JJ (2004) Use of spectroscopic techniques for uranium(VI)/montmorillonite interaction modeling. *Environ Sci Technol* 38:1399–1407. <https://doi.org/10.1021/es0348344>
- Kremleva A, Krüger S, Rösch N (2008) Density functional model studies of uranyl adsorption on (001) surfaces of kaolinite. *Langmuir* 24:9515–9524. <https://doi.org/10.1021/la801278j>
- Krepelova A, Brendler V, Sachs S et al (2007) U(VI)-kaolinite surface complexation in absence and presence of humic acid studied by TRLFS. *Environ Sci Technol* 41:6142–6147
- Li D, Kaplan DI (2012) Sorption coefficients and molecular mechanisms of Pu, U, Np, Am and Tc to Fe (hydr)oxides: a review. *J Hazard Mater* 243:1–18. <https://doi.org/10.1016/j.jhazmat.2012.09.011>
- Li D, Seaman JC, Chang H-S et al (2014) Retention and chemical speciation of uranium in an oxidized wetland sediment from the

- Savannah River Site. *J Environ Radioact* 131:40–46. <https://doi.org/10.1016/j.jenvrad.2013.10.017>
- Liu GJ, Zhang XR, McWilliams L et al (2008) Influence of ionic strength, electrolyte type, and NOM on As(V) adsorption onto TiO₂. *J Environ Sci Health Part A* 43:430–436. <https://doi.org/10.1080/10934520701795749>
- Mahoney JJ, Cadle SA, Jakubowski RT (2009) Uranyl adsorption onto hydrous ferric oxide—a re-evaluation for the diffuse layer model database. *Environ Sci Technol* 43:9260–9266. <https://doi.org/10.1021/es901586w>
- Missana T, García-Gutiérrez M, Maffiotte C (2003) Experimental and modeling study of the uranium (VI) sorption on goethite. *J Colloid Interface Sci* 260:291–301
- Nair S, Karimzadeh L, Merkel BJ (2014) Surface complexation modeling of uranium(VI) sorption on quartz in the presence and absence of alkaline earth metals. *Environ Earth Sci* 71:1737–1745. <https://doi.org/10.1007/s12665-013-2579-5>
- O’Loughlin EJ, Boyanov MI, Antonopoulos DA, Kemner KM (2011) Redox processes affecting the speciation of technetium, uranium, neptunium, and plutonium in aquatic and terrestrial environments. In: *Aquatic redox chemistry*. American Chemical Society, pp 477–517
- Pabalan RT, Turner DR (1996) Uranium(6+) sorption on montmorillonite: experimental and surface complexation modeling study. *Aquat Geochem* 2:203–226. <https://doi.org/10.1007/BF01160043>
- Parkhurst DL, Appelo CA (1999) User’s guide to PHREEQC (version 2)—a computer program for speciation, reaction-path, 1D-transport, and inverse geochemical calculations. US Geological Survey
- Payne TE, Davis JA, Lumpkin GR et al (2004) Surface complexation model of uranyl sorption on Georgia kaolinite. *Appl Clay Sci* 26:151–162. <https://doi.org/10.1016/j.clay.2003.08.013>
- Prikryl JD, Jain A, Turner DR, Pabalan RT (2001) Uranium(VI) sorption behavior on silicate mineral mixtures. *J Contam Hydrol* 47:241–253
- Riley RG, Zachara JM, Wobber FJ (1992) Chemical contaminants on DOE lands and selection of contaminant mixtures for subsurface science research. DOE, Washington
- Schwertmann U, Cornell RM (1991) Iron oxides in the laboratory—preparation and characterization. VCH Verlagsgesellschaft, Weinheim; 137 Seiten, 40 Abbildungen, 4 Tabellen, Hardcover, 118,-DM. ISBN 3-527-26991-6
- Sherman DM, Peacock CL, Hubbard CG (2008) Surface complexation of U(VI) on goethite (α -FeOOH). *Geochim Cosmochim Acta* 72:298–310. <https://doi.org/10.1016/j.gca.2007.10.023>
- Stoliker DL, Kent DB, Zachara JM (2011) Quantifying differences in the impact of variable chemistry on equilibrium uranium(VI) adsorption properties of aquifer sediments. *Environ Sci Technol* 45:8733–8740. <https://doi.org/10.1021/es202677v>
- Sverjensky DA (2003) Standard states for the activities of mineral surface sites and species. *Geochim Cosmochim Acta* 67:17–28. [https://doi.org/10.1016/S0016-7037\(02\)01074-8](https://doi.org/10.1016/S0016-7037(02)01074-8)
- Sze A, Erickson D, Ren L, Li D (2003) Zeta-potential measurement using the Smoluchowski equation and the slope of the current–time relationship in electroosmotic flow. *J Colloid Interface Sci* 261:402–410. [https://doi.org/10.1016/S0021-9797\(03\)00142-5](https://doi.org/10.1016/S0021-9797(03)00142-5)
- Tapia-Rodríguez A, Luna-Velasco A, Field JA, Sierra-Alvarez R (2012) Toxicity of uranium to microbial communities in anaerobic biofilms. *Water Air Soil Pollut* 223:3859–3868. <https://doi.org/10.1007/s11270-012-1154-0>
- Turner DR, Sassman SA (1996) Approaches to sorption modeling for high-level waste performance assessment. *J Contam Hydrol* 21:311–332. [https://doi.org/10.1016/0169-7722\(95\)00056-9](https://doi.org/10.1016/0169-7722(95)00056-9)
- Um W, Serne RJ, Brown CF, Rod KA (2008) Uranium(VI) sorption on iron oxides in Hanford Site sediment: application of a surface complexation model. *Appl Geochem* 23:2649–2657. <https://doi.org/10.1016/j.apgeochem.2008.05.013>
- USEPA (2014) Method 6020B, rev. 2. Inductively coupled plasma-mass spectrometry, test methods for evaluating solid waste. U.S. Gov. Print. Office
- Uyuşur B, Li C, Baveye PC, Darnault CJG (2014) pH-dependent reactive transport of uranium(VI) in unsaturated sand. *J Soils Sediments* 15:634–647. <https://doi.org/10.1007/s11368-014-1018-x>
- Waite TD, Davis JA, Payne TE et al (1994) Uranium(VI) adsorption to ferrihydrite: application of a surface complexation model. *Geochim Cosmochim Acta* 58:5465–5478. [https://doi.org/10.1016/0016-7037\(94\)90243-7](https://doi.org/10.1016/0016-7037(94)90243-7)
- Wang Z, Ulrich K-U, Pan C, Giammar DE (2015) Measurement and modeling of U(IV) adsorption to metal oxide minerals. *Environ Sci Technol Lett* 2:227–232. <https://doi.org/10.1021/acs.estlett.5b00156>
- Westall J (1985) A program for the determination of chemical equilibrium constants from experimental data: user’s guide. Department of Chemistry, Oregon State University, Corvallis
- Whittig LD, Allardice WR (1986) X-ray diffraction techniques. In: *Methods of soil analysis, part 1. Physical and mineralogical methods*. ASA, pp 331–362
- Zachara JM, Long PE, Bargar J, Davis JA, Fox PM, Fredrickson JK, Freshley MD, Konopka A, Liu C, McKinley JP, Rockhold ML, Williams KH, Yabusaki SB (2013) Persistence of uranium groundwater plumes: contrasting mechanisms at two DOE sites in the groundwater–river interaction zone. *J Contam Hydrol* 147:45–72. <https://doi.org/10.1016/j.jconhyd.2013.02.001>